

Carbon Nanotubes as Electrodes for Dielectrophoresis of DNA

Sampo Tuukkanen, J. Jussi Toppari, Anton Kuzyk, Lasse Hirviniemi, Vesa P. Hytönen^{†,‡}, Teemu Ihalainen[†], and Päivi Törmä*

Nanoscience Center, Department of Physics and [†]Department of Biological and Environmental Science, University of Jyväskylä, P.O.Box 35 (YN), FIN-40014 Jyväskylä, Finland, and [‡]Present address: Department of Materials, ETH Zürich, Hönggerberg, CH-8093 Zürich, Switzerland.

*E-mail: paivi.torma@phys.jyu.fi.

ABSTRACT

Dielectrophoresis can potentially be used as an efficient trapping tool in the fabrication of molecular devices. For nanoscale objects, however, the Brownian motion poses a challenge. We show that the use of carbon nanotube electrodes makes it possible to apply relatively low trapping voltages and still achieve high enough field gradients for trapping nanoscale objects, e.g., single molecules. We compare the efficiency and other characteristics of dielectrophoresis between carbon nanotube electrodes and lithographically fabricated metallic electrodes, in the case of trapping nanoscale DNA molecules. The results are analyzed using finite element method simulations and reveal information about the frequency dependent polarizability of DNA.

Controlled assembly of nanoscale objects is a prerequisite for the realization of molecular devices. Self-assembly, nanolithographic methods, and manipulation with electromagnetic fields are the promising candidates to achieve this goal, and it is likely that they will be used together, in a complementary way, in the assembly process. Dielectrophoresis (DEP),¹ the movement of polarizable particle induced by a nonhomogenous electric field, is an electronic analogue of optical tweezers.² DEP has already been demonstrated to be useful in many different fields,^{3,4} e.g., for separation of metallic carbon nanotubes from semiconducting ones.⁵ Due to its nondestructive nature, DEP has been widely used as an active manipulation method, especially for trapping biological micrometer-scale objects such as cells,^{6,7} bacterial species,⁸ and various size DNA,⁹ and also in nanoscale for individual proteins.¹⁰ In this Letter, we present the first demonstration of DEP of nanoscale molecules (short DNA) using a carbon nanotube (CNT) as an electrode. We quantitatively verify the superior performance of CNT electrodes compared to lithographically fabricated nanoelectrodes and analyze the data by finite-element method simulations, obtaining information about the polarizability of DNA.

The dielectrophoretic force, $F_{\text{DEP}} = \alpha \nabla(E^2)$, is determined by the magnitude of electric field gradient and particle polarizability α . For nanoscale objects, the increase in Brownian motion requires higher field gradients to realize the trapping. An obvious way to achieve higher gradients would be to increase the voltage. However, to avoid unfavorable electrochemical effects and to minimize

disturbing convectional flows, caused by the electrohydrodynamic effects and medium heating,¹¹ trapping voltages should be kept sufficiently low. The other option to achieve high gradients is to make electrodes smaller. This method has so far been successfully applied to trap, e.g., single DNA molecules of the length scale of ~ 100 nm.¹²⁻¹⁴ Nowadays, lithographically fabricated electrodes have a minimum line width of tens of nanometers. These structures do not offer large enough electric field gradients to overcome Brownian motion of less than ~ 10 nm sized objects, when sufficiently low voltages are used. Since a single-walled carbon nanotube (SWCNT) is only about 1 nm in diameter, and a few nanometers in the case of multiwalled carbon nanotubes (MWCNTs), they can be used as electrodes to form very high electric field gradients, as suggested by Burke.³ In pioneering experiments toward this, CNTs which were either bridging the metal electrodes or having at least a few micrometer gap to the other electrode, were used for DEP of polystyrene and gold nanoparticles.¹⁵ The nanoparticles were observed to immobilize along the whole nanotube, since the electric field gradient is large everywhere near the nanotube. Using present fabrication methods, e.g., focused ion-beam cutting and/or tens of nanometers accurate alignment off the e-beam lithography pattern (in our case), one can obtain a nanoscale gap also in the case of carbon nanotube electrodes.¹⁶ In this Letter, we demonstrate for the first time the trapping of DNA molecules, of ~ 50 and ~ 360 nm in contour length, to the end of a carbon nanotube which has 100 nm scale separation from a metal electrode.

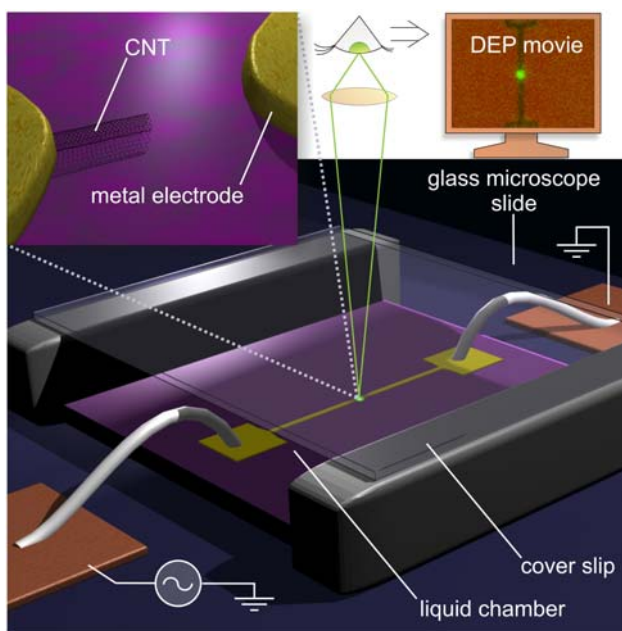


Figure 1. A schematic view of the experimental setup used in the DEP experiments under the confocal microscope. The solution containing DNA is in the moisture chamber between the silicon substrate and the cover slip. The structure with carbon nanotube as one electrode is presented in the close-up image. Repeated confocal microscope images are captured to obtain time-resolved information about the DEP process (the “DEP movie”).

Quantitative analysis of the trapping process is done using in situ confocal fluorescence microscopy. Our analysis reveals information about DNA polarizability as a function of frequency which is essential, e.g., for applications utilizing DEP based trapping and manipulation of DNA. The remarkable self-assembly properties of DNA, for instance the recent development of “DNA origami”,¹⁷ makes it a potential tool for self-assembly of molecular electronics circuits.

To obtain the nanotube electrode structure (see Figure 1), a mixture of MWCNTs¹⁸ in powder form was dissolved in 1,2-dichloroethane by diluting and sonicating several times. The mixture was spun on the substrate (300 μm thick silicon wafer with 700 nm Si_3N_4 on both sides). After spinning, samples were imaged with atomic force microscopy (AFM) and scanning electron microscopy (SEM). The substrate had a prefabricated metallic mark grid which was used for the stage alignment in SEM when making contacts to the nanotubes. The contacts were made using standard e-beam lithography and evaporation of metal (2–5 nm Ti followed by 15 nm Au) in an ultrahigh vacuum (UHV) chamber. Some of the contacted nanotubes were too weakly conducting (semiconducting) for DEP experiments. To compare the efficiency of the trapping process, we used also finger-tip type metal electrodes (the schematic structure can be seen in Figure 2d) fabricated using e-beam lithography and UHV evaporation (2–5 nm Ti and 15 nm Au).

Double-stranded DNA (dsDNA) fragments (145 bp and 1065 bp) were fabricated by polymerase chain reaction (PCR) using appropriate primers and by digestion of

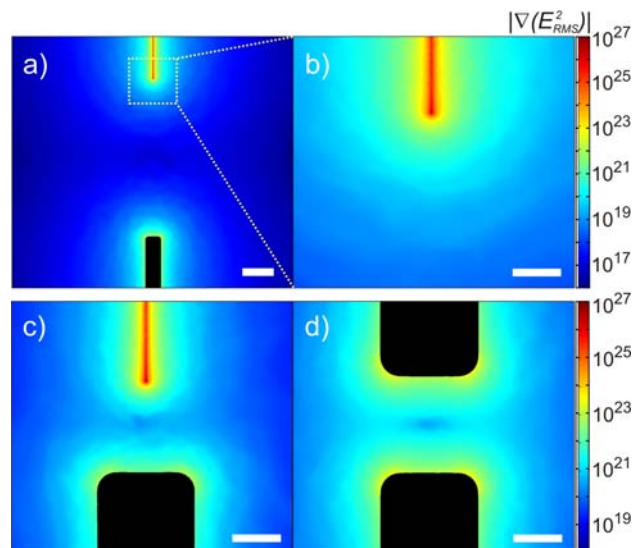


Figure 2. Contour plot of the gradient of the field square, $\nabla(E_{\text{rms}}^2)$, in the plane 2 nm above the substrate surface, i.e., 0.2 nm above the CNT in (a–c). The DEP force has the maximum value in the very end of the CNT in (a–c). In (a), and the close-up (b), the gap size is 1 μm and in (c) and (d) the gap size is 100 nm. The dc voltage between the electrodes is 1.6 V_{rms} . The scale bars are 200 nm in (a) and 50 nm in (b–d).

pBVboostFG¹⁹ plasmids with restriction enzymes BglI & SpeI (Promega), respectively, following purification with agarose gel electrophoresis and ion exchange chromatography. Prior to use, DNA fragments were diluted into buffer containing 3 mM Hepes and 1 mM NaOH (pH 6.9). The buffer conductivity was measured to be 20 $\mu\text{S}/\text{cm}$: low enough to ensure good performance of DEP.²⁰ The DNA was labeled with dsDNA specific fluorescent label PicoGreen (Molecular Probes). PicoGreen stock solution was first diluted 1:100 into 3 mM Hepes and 1 mM NaOH buffer and then mixed 1:1 with the DNA solution to get the final solution. The final DNA concentrations were 58 nM (145 bp) and 8 nM (1065 bp), chosen so that the concentration of the nucleotides remains the same. The final concentration of PicoGreen was 1.6 μM yielding a dye to base pair ratio of 1:5.²¹

Dielectrophoresis experiments under the confocal microscope (Zeiss Axiovert LSM510, Zeiss “Fluar” 40x/1.3 Oil objective) were performed by (fluorescent) imaging of $10 \times 10 \mu\text{m}^2$ square area around the gap (constriction between the electrodes), during the trapping of molecules using an ac signal applied to the electrodes. Image data were collected simultaneously from two channels: the fluorescence channel, which corresponds to the amount of DNA, and the reflection channel, which shows the location of the electrodes. Time-resolved data, i.e., dielectrophoresis movies were obtained by capturing two 128×128 pixel frames per second. For imaging, an argon laser (488 nm) with power of 0.45 mW was used, and also tested in advance so as not to induce bleaching of the PicoGreen dye. In the beginning of a DEP movie, the voltage is kept off for 10 s after which the sinusoidal ac signal is turned on (to a certain starting voltage value). The voltage was raised 0.2 $V_{\text{p-p}}$ (0.07 V_{rms}) after each 20 s period until the final voltage

value was reached. The voltage was then turned off but the data collection was continued for 20 seconds to observe how DNA diffuses away from the gap.

For the analysis, the collected amount of DNA in the gap was obtained from the fluorescence movie by determining the mean fluorescence intensity inside the circle shaped (diameter of 1.6 μm) area in the gap between finger-tip electrodes (or at the end of CNT) subtracted by the mean intensity of the background fluorescence (measured from the circle shaped area on substrate surface a few μm distance from the gap). To maximize the detector sensitivity, the detector gain and amplification offset were fine-tuned according to the fluorescence background of each sample. This was needed to be able to distinguish from the background small changes in fluorescence due to DNA. However, this makes (for technical reasons) the absolute fluorescence values not exactly comparable to each other. Therefore, the obtained fluorescence curves were normalized by setting the maximum fluorescence intensity observed for each sample to unity. Note that even when the absolute intensities are not directly available, we obtain a lot of consistent information about the frequency and voltage dependence of the trapping process. Especially, the measurement is optimized for obtaining accurate information about the minimum voltage V_{min} for which the trapping begins, which is the important quantity on which our main conclusions are based.

The data analysis was accompanied by finite element method simulations by Comsol Multiphysics software, which was used to simulate the electric field (using dc voltage) in three dimensions for two nanoelectrode configurations: (1) two finger-tip type electrodes and (2) a finger-tip type and a CNT electrode (see Figure 1). For the 1 μm buffer layer, we used the permittivity of water, $\epsilon_m = 80$, which is a good approximation for our dilute Hepes buffer. Under the electrodes, there was a 700 nm layer of Si_3N_4 ($\epsilon_r = 6.0$) and 300 nm layer of silicon ($\epsilon_r = 11.7$). The values for relative permittivities were chosen to correspond to the situation of using a 1 MHz electric field. The gradient of the electric field square $\nabla(E^2)$, from which one can get the DEP force $F_{DEP} = \alpha \nabla(E^2)$ (E is the root mean square value of the electric field assuming a sinusoidal time dependence¹) by multiplying with the effective polarizability of the molecule α , is plotted in Figure 2.

In the following, we will demonstrate that carbon nanotubes indeed function efficiently as electrodes for DEP. It is shown by simulations and experiments that the trapping efficiency in case of carbon nanotube electrodes considerably exceeds that of the 100 nm size metal electrodes. By combining the information from the experiments and the simulations, we also obtain the values for frequency dependence of DNA polarisability.

The CNT electrode sample shown in Figure 3 was used to trap 1065 bp DNA. DNA is collected to the end of the nanotube, where the DEP force is at its maximum (see Figure 2), and not to the end of the metal electrode or in the middle of the gap. In the metal electrode sample, the gap size was ~ 100 nm, whereas in the case of the CNT

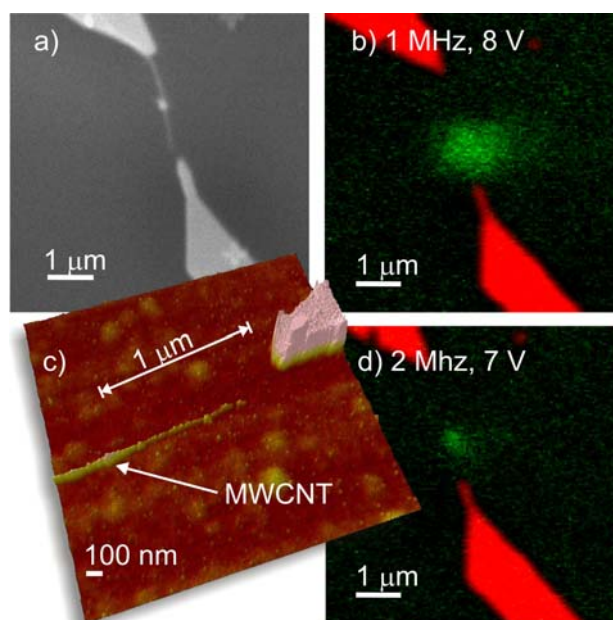


Figure 3. DEP of 1065 bp dsDNA using CNT as one electrode: (a) SEM and (c) AFM images of the multiwalled CNT electrode sample before confocal experiment. (b) and (d) show the trapped DNA spot when a certain frequency and voltage were used.

electrode sample it was ~ 400 nm (see the AFM image in Figure 3c). However, in the fluorescence images (parts b and d of Figure 3), the fluorescence spot is not located exactly at the end of the nanotube as it appears in the AFM image, but rather about 1 μm from the metal electrode. From the AFM image, one can see that the MWCNT gets narrower and clumpy near to its end and the conformation appears deformed. The “real end” of the MWCNT is thereby at ~ 1 μm distance from the metal electrode. This means that the DEP can also be used for characterization of CNT and other ultrathin nanowires.

When using 145 bp DNA, the expected behavior, i.e., DNA collected to the CNT, was observed in two different CNT electrode samples, shown in Figure 4. In contrast to the sample used in the case of 1065 bp DNA, which clearly collected DNA on the whole frequency range, i.e., from 0.1 to 10 MHz, in the samples used for 145 bp DNA the collecting to the CNT was not clearly seen in the whole frequency range but was most efficient at 5 MHz frequency. This is because the metal electrodes of the samples (Figure 4) are quite close to the CNT end and collect, for lower frequencies, some DNA to the metal electrode edges (due to the high field gradients on the rough edges) which decreases fluorescence contrast.

For quantitative analysis, the fluorescence as a function of the DEP voltage and frequency was studied. The fluorescence intensity of captured DNA as a function of the average electric field strength in the cases of CNT and metal electrode is shown in Figure 5. One can see that higher electric fields are needed for trapping DNA in the case of the metal fingertip electrode, which is consistent with the simulation results in Figure 2 where the DEP force is much larger near the CNT end than near the fingertip

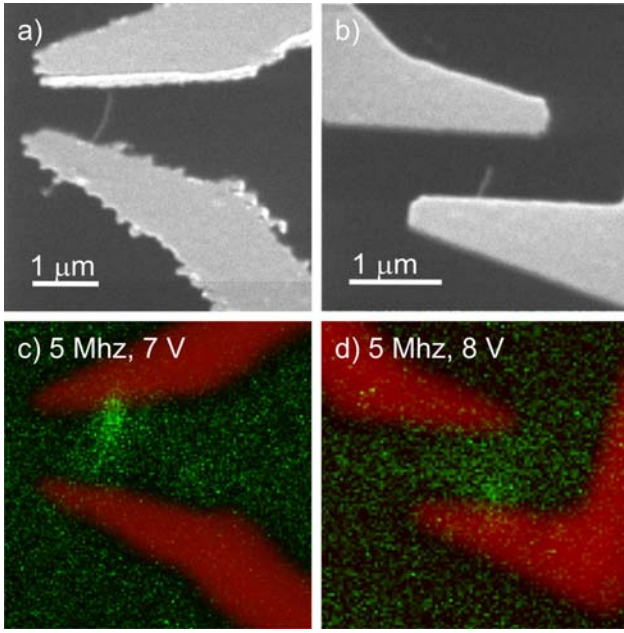


Figure 4. DEP of 145 bp dsDNA using CNT as an electrode. (a) and (b) are SEM images of the CNT electrode samples and (c) and (d) are corresponding fluorescence images taken during the DEP, using the shown frequency and voltage. The gap sizes are in (a) ~ 115 nm and in (b) ~ 350 nm.

electrode – even in the case of the $1 \mu\text{m}$ gap (Figure 2b). CNT works as an effective DEP trap, even if the CNT end is far from the other electrode. The higher efficiency of the trapping in the case of CNT electrode makes it also more sensitive to the frequency used in the DEP process, which allows us to obtain the frequency dependency of the DNA polarizability. By the trapping efficiency, we mean the following: how low field strengths are sufficient for trapping? Especially, we use the minimum voltage V_{\min} , and the corresponding field strength, for which the trapping begins for determining this. That is, the lower the $V_{\min}/$ the field strength, the higher the trapping efficiency.

The DEP potential energy for polarizable, uncharged molecule in applied electric field $\bar{E}(\bar{r})$ is $U_{\text{DEP}}(\bar{r}, \omega) = -\frac{1}{2}\alpha E^2$, where the effective polarizability α depends on the frequency ω of the applied signal and on the size of the molecule. On the other hand, Brownian motion is associated with the thermal energy $U_{\text{th}} = \frac{1}{2}k_{\text{B}}T$. The use of an ac field averages the electrophoretic forces acting on DNA to zero and we obtain for the total potential energy $U_{\text{tot}} = U_{\text{DEP}} + U_{\text{th}}$, which has a minimum at the point of highest electric field. By determining experimentally the minimum electric field needed to trap a certain size molecule, one can calculate its polarizability α .

To calculate polarizability of 1065 bp DNA from the experimental data, shown in Figure 5a, we first determined the minimum voltage V_{\min} needed to collect the smallest observable amount of DNA to the DEP trap. This was done by fitting the fluorescence intensity to the function $I = I_0 + A(V^b + V_{\min}^b)^{2/b}$ which produces V^2 dependency after the voltage V_{\min} has been reached (dotted lines in Fig. 5a). The V^2 dependency is physically motivated by the DEP force,

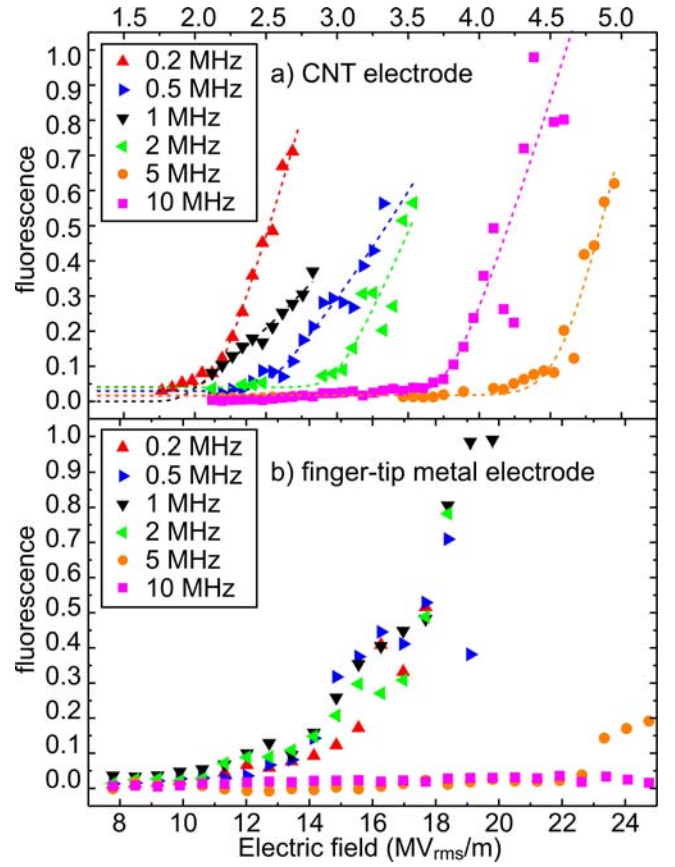


Figure 5. Comparison of the trapping efficiency of CNT electrode vs finger-tip electrodes. The curves show the fluorescence (a) in the end of CNT (with electrode separation $d = 1 \mu\text{m}$) and (b) in the gap (in the case of finger-tip metal electrodes separation $d = 100$ nm) as a function of the electric field (an average electric field strength between the electrodes, $E = V/d$). Dotted lines in (a) are fits to the data using the function $I = I_0 + A(V^b + V_{\min}^b)^{2/b}$ (see text). By comparing the field strength needed to trap DNA in these cases, one can clearly see that CNT electrode shows better performance than lithographically fabricated nanoelectrodes.

$F_{\text{DEP}} = 2\alpha E V E$, and has also been observed experimentally in ref. 22. The parameter b determines the rate of the asymptotic change from constant value (~ 0) to V^2 dependency (the best fit was found using $b = 40$). Next, we performed simulations using the obtained voltage V_{\min} , to find out the electric field strength E_{\min} on the edge of the observed fluorescence spot, i.e., on the edge of the DEP trap. For all frequencies, the radius for the observable fluorescence spot in confocal microscope image was $r = (0.5 \pm 0.1) \mu\text{m}$. Thus, E_{\min} was read from the simulation at the distance r from the CNT end, perpendicular to it, in the plane parallel to the substrate, 0.2 nm above the CNT. Now, setting the total potential to zero ($U_{\text{tot}} = 0$) on the edge of the fluorescence spot, we obtain the polarizability as $\alpha = 3k_{\text{B}}T/E_{\min}^2$. Normalized polarizability (polarizability divided by the molecule length in base pairs) as a function of frequency is shown in Figure 6 together with values from the literature for various size DNA molecules.^{20,23,24}

We observed that the polarizability of DNA decreases with the increase of frequency (see Figure 6), which has also been shown earlier, e.g., for 12 kbp plasmid DNA.²³ In

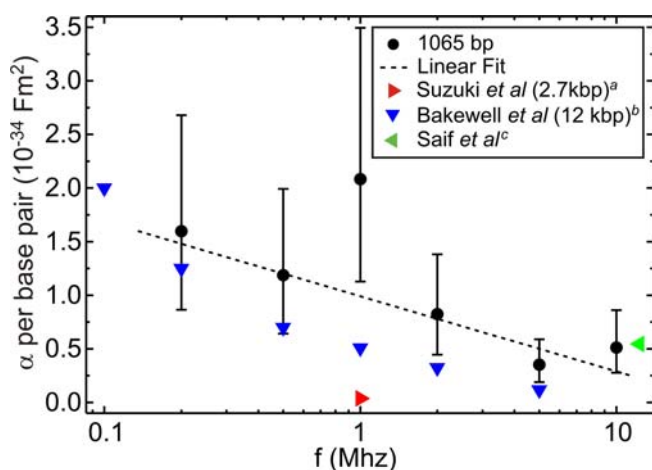


Figure 6. Polarizability of 1065 bp DNA calculated from the fluorescence data captured during DEP using CNT electrode sample shown in Figure 3. The error bars originate from the uncertainty of the observed fluorescence spot radius ($0.5 \pm 0.1 \mu\text{m}$). Other values are taken from refs ^a20, ^b23, and ^c24.

addition, the polarizability of calf thymus DNA²⁴ corresponds well to our observed 10 MHz value even when the DNA they used was much longer. However, the value ($\alpha = 10^{-32} \text{ F m}^2$) obtained for 2.7 kbp plasmid DNA²⁰ using fluorescence anisotropy measurements is about 1 magnitude smaller than the others. The similarity of the polarizability results in the case of different size DNAs can be understood by Manning's model,²⁵ where the counterions move freely along the macromolecular "DNA subunit" length. Since each subunit gives a contribution to the polarizability of the whole molecule, total polarizability divided by the DNA size should remain constant. However, the length of the subunit depends, e.g., on the DNA concentration.²⁶ Differences between experiments may also be caused by differences in buffer, e.g., viscosity,¹³ or DNA length and shape: plasmid has circular conformation and also globular shape secondary structure, which limits its unwinding and stretching during DEP²⁰ and thus lowers the final polarizability compared to DNA fragments.

In summary, we have shown that the use of CNT as an electrode for dielectrophoretic trapping of nanometer scale DNA molecules gives significantly better performance compared to lithographically fabricated 100 nm wide fingertip type nanoelectrodes, even when the gap is larger in the case of the CNT sample. The polarizability of 1065 bp DNA was calculated using the data obtained from in situ confocal microscope studies of DNA dielectrophoresis. Comparison of the polarizability values and their frequency dependence to values obtained from the literature indicates simple scalability in the size-dependence of the polarizability. Further studies are needed concerning the frequency and the size dependence of DNA DEP efficiency to find out whether it could be used even to separate

molecules by their size, and therefore be used for molecular electronics device fabrication in a more sophisticated manner.

Acknowledgement. We acknowledge the financial support by the Academy of Finland and EUROHORCS (EURYI Award, Academy Project Number 205470), the National Graduate School in Informational and Structural Biology, and the National Graduate School in NanoScience.

References

- (1) Pohl, H. A. *J. Appl. Phys.* **1951**, *22*, 869-871; Pohl, H. A. *Dielectrophoresis: The Behavior of Neutral Matter in Nonuniform Electric Fields*; Cambridge University Press: Cambridge, U.K., 1978.
- (2) Ashkin, A.; Dziedzic, J. M.; Bjorkholm, J. E.; Chu, S. *Opt. Lett.* **1986**, *11*, 288.
- (3) Burke, P. J.; *Encycl. Nanosci. Nanotechnol.*, **2004**, *6*, 623.
- (4) Hughes, M. P. *Nanotechnology* **2000**, *11*, 124.
- (5) Krupke, R.; Hennrich, F.; v. Löhneysen, H.; Kappes, M. M. *Science* **2003**, *301*, 344.
- (6) Masuda, S.; Washizu, M.; Nanba, T. *IEEE Trans. Indust. Appl.* **1989**, *25*, 732; Washizu, M.; Nanba, T.; Masuda, S. *IEEE Trans. Indust. Appl.* **1990**, *26*, 352.
- (7) Becker, F. F.; Wang, X.-B.; Huang, Y.; Pethig, R.; Vykoukal, J.; Gascoyne, P. R. C. *J. Phys. D: Appl. Phys.* **1994**, *27*, 2659.
- (8) Markx, G. H.; Huang, Y.; Zhou, X. F.; Pethig, R. *Microbiology* **1994**, *140*, 585; Markx, G. H.; Pethig, R. *Biotechnol. Bioeng.* **1995**, *45*, 337.
- (9) Hölzel, R.; Bier, F. F. *IEE Proc.-Nanobiotechnol.* **2003**, *150*, 47.
- (10) Hölzel, R.; Calander, N.; Chiragwandi, Z.; Willander, M.; Bier, F. F. *Phys. Rev. Lett.* **2005**, *95*, 128102.
- (11) Castellanos, A.; Ramos, A.; González, A.; Green, N. G.; Morgan, H. J. *J. Phys. D: Appl. Phys.* **2003**, *36*, 2584.
- (12) Tuukkanen, S.; Kuzyk, A.; Toppari, J. J.; Hytönen, V. P.; Ihalainen, T.; Törmä, P. *Appl. Phys. Lett.* **2005**, *87*, 183102.
- (13) Chou, C.-F.; Tegenfeldt, J.; Bakajin, O.; Chan, S. S.; Cox, E. C.; Darnton, N.; Duke, T.; Austin, R. H. *Biophys. J.* **2002**, *83*, 2170.
- (14) Ying, L.; White, S. S.; Bruckbauer, A.; Meadows, L.; Korchev, Y. E.; Klenerman, D. *Biophys. J.* **2004**, *86*, 1018.
- (15) Zheng, L.; Li, S.; Brody, J. P.; Burke, P. J. *Langmuir* **2004**, *20*, 8612.
- (16) Sasaki, T. K.; Ikegami, A.; Mochizuki, M.; Aoki, N.; Ochiai, Y. *IPAP Conf. Series* **2005**, *6*, 171.
- (17) Rothmund, P. W. K. *Nature* **2006**, *440*, 297.
- (18) Nanotubes were made by the group of S. Iijima according to the recipe given in: Koshio, A.; Yudasaka, M.; Iijima, S. *Chem. Phys. Lett.* **2002**, *356*, 595.
- (19) Laitinen, O. H.; Airene, K. J.; Hytönen, V. P.; Peltomaa, E.; Mähönen, A. J.; Wirth, T.; Lind, M. M.; Mäkelä, K. A.; Toivanen, P. I.; Schenkwein, D.; Heikura, T.; Nordlund, H. R.; Kulomaa, M. S.; Ylä-Herttua, S. *Nucleic Acids Res.* **2005**, *33*, e42.
- (20) Suzuki, S.; Yamanashi, T.; Tazawa, S.; Kurosawa, O.; Washizu, M. *IEEE Trans. Ind. Appl.* **1998**, *34*(1), 75.
- (21) Singer, V. L.; Jin, X.; Jones, L.; Yue, S.; Haugland, R. P. *Biotechnology International* **1997**, *1*, 267.
- (22) Asbury, C. L.; Diercks, A. H.; van den Engh, G. *Electrophoresis* **2002**, *23*, 2658.
- (23) Bakewell, D. J.; Morgan, H. *IEEE Trans. NanoBiosci.* **2006**, *5*, 1.
- (24) Saif B, Mohr RK, Montrose CJ and Litovitz TA *Biopolymers* **1991**, *31*, 1171.
- (25) Manning, G. S. *Q. Rev. Biophys.* **1978**, *11*, 179.
- (26) Bone, S.; Lee, R. S.; Hodgson, C. E. *Biochim. Biophys. Acta* **1996**, *1306*, 93.